Biomaterials Science

ROYAL SOCIETY OF CHEMISTRY

PAPER

View Article Online
View Journal | View Issue

Cite this: *Biomater. Sci.*, 2025, **13**, 434

Metabolic labeling and targeted modulation of adipocytes†

Yueji Wang,‡[a,b] Yang Bo,‡[a] Yusheng Liu,[a] Jiadiao Zhou,[a] Daniel Nguyen,[a] Dhyanesh Baskaran,[a] Yuan Liu[a] and Hua Wang *[a,c,d,e,f,g,h]

Received 11th October 2024,
Accepted 27th November 2024

DOI: 10.1039/d4bm01352b

rsc.li/biomaterials-science

Adipocytes play a critical role in energy storage and endocrine signaling and are associated with various diseases such as cancer and diabetes. Facile strategies to engineer adipocytes have long been pursued for elucidating adipocyte biology and developing adipocyte-based therapies. Herein, we report metabolic glycan labeling of adipocytes and subsequent targeted modulation of adipocytes *via* click chemistry. We show that azido tags expressed on the surface of adipocytes can persist for over 4 days. By conjugating dibenzocyclooctyne (DBCO)-cargos onto azido-labeled adipocytes *via* click chemistry, the cargos can be retained on the adipocyte membrane for over 12 hours. We further show that signaling molecules including adiponectin, calreticulin, mannose-binding lectin 2, and milk fat globule-EGF factor 8 protein can be conjugated to adipocytes to orchestrate their phagocytosis by macrophages. The azido-labeled adipocytes grafted into mice can also mediate targeted conjugation of DBCO-cargos *in vivo*. This adipocyte labeling and targeting technology will facilitate the development of adipocyte-based therapies and provides a new platform for manipulating the interaction between adipocytes and other types of cells.

Introduction

Adipocytes play a critical role in energy storage and endocrine signaling and are often associated with diseases such as cancer and diabetes.[1–4] For example, cancer-associated adipocytes could contribute to the growth, metastasis, and drug resistance of tumor cells.[5–7] White adipocytes rich in fatty acids are also a key target of obesity-control measures and diabetes therapies.[8,9] While current approaches focus on eliminating or transforming adipocytes to facilitate disease control, the potential of adipocytes themselves for therapy has not been well explored. Adipocytes are abundant in the body, can be easily identified and isolated, and are lowly immunogenic, providing an ideal source of biocompatible materials for drug delivery and transplantation applications.[10,11] Indeed, adipose tissue transplantation has been used in the context of breast cancer surgery in the clinic as a means to facilitate breast reconstruction post-surgery.[12,13] Adipocyte-based cell therapies for controlling obesity and treating type-1 diabetes are also actively pursued.[14,15] These applications often necessitate the surface engineering of adipocytes or the incorporation of cargos into adipocytes, but are limited by the lack of facile methods to functionalize adipocytes.

Metabolic glycan labeling, by taking advantage of glycoengineering processes of unnatural sugars, provides a powerful tool to label cell-surface glycoproteins and glycolipids with unique chemical tags (*e.g.*, azido groups),[16–21] for subsequent targeted conjugation of dibenzocyclooctyne (DBCO)-bearing agents *via* efficient click chemistry.[22–24] While metabolic glycan labeling of cancer cells, bacteria, and immune cells has been extensively studied and has enabled the development of various cell-targeted diagnostics and therapies,[25–32] metabolic glycan labeling of adipocytes with a low proliferative ability and distinct metabolism remains poorly understood. Here, we carefully examined the metabolic glycan labeling kinetics of adipocytes and the stability of expressed chemical tags (*e.g.*, azido groups) over time. The targeting efficiency of DBCO-agents towards azido-labeled adipocytes as well as the retention time of the conjugated agents on the surface of adipocytes

[a]*Department of Materials Science and Engineering, University of Illinois at Urbana-Champaign, Urbana, IL 61801, USA. E-mail: huawang3@illinois.edu*
[b]*Department of Mechanical Science and Engineering, University of Illinois at Urbana-Champaign, Urbana, IL 61801, USA*
[c]*Cancer Center at Illinois (CCIL), Urbana, IL 61801, USA*
[d]*Institute for Genomic Biology, University of Illinois at Urbana-Champaign, Urbana, IL 61801, USA*
[e]*Department of Bioengineering, University of Illinois at Urbana-Champaign, Urbana, IL 61801, USA*
[f]*Carle College of Medicine, University of Illinois at Urbana-Champaign, Urbana, IL 61801, USA*
[g]*Beckman Institute for Advanced Science and Technology, University of Illinois at Urbana-Champaign, Urbana, IL 61801, USA*
[h]*Materials Research Laboratory, University of Illinois at Urbana-Champaign, Urbana, IL 61801, USA*

†Electronic supplementary information (ESI) available. See DOI: **https://doi.org/10.1039/d4bm01352b**

‡These authors contributed equally to this work.

have also been studied. This adipocyte labeling and targeting technology provides a facile approach for engineering adipocytes, and holds tremendous promise for targeted delivery of diagnostic and therapeutic agents to adoptively transferred adipocytes *in vivo*.

The interactions between adipocytes and immune cells such as macrophages are deemed crucial for the homeostasis of adipose tissues and other tissues. For example, macrophages can infiltrate adipose tissues, recognize and bind to apoptotic adipocytes, and eventually phagocytose and break down the dead or dying adipocytes. In healthy individuals, the phagocytosis of adipocytes by macrophages is considered a normal homeostatic process that aids in maintaining adipose tissue integrity and function.[33–36] In the context of obesity and metabolic disorders, the excessive phagocytosis of adipocytes by macrophages could result in the release of pro-inflammatory cytokines to exacerbate adipose tissue inflammation and insulin resistance.[37–39] Extensive research has been performed to date to uncover and further modulate the phagocytotic process of adipocytes by macrophages, and has suggested the important role of various types of cytokines and cell-surface signaling molecules (*e.g.*, CD47, calreticulin, and adiponectin)

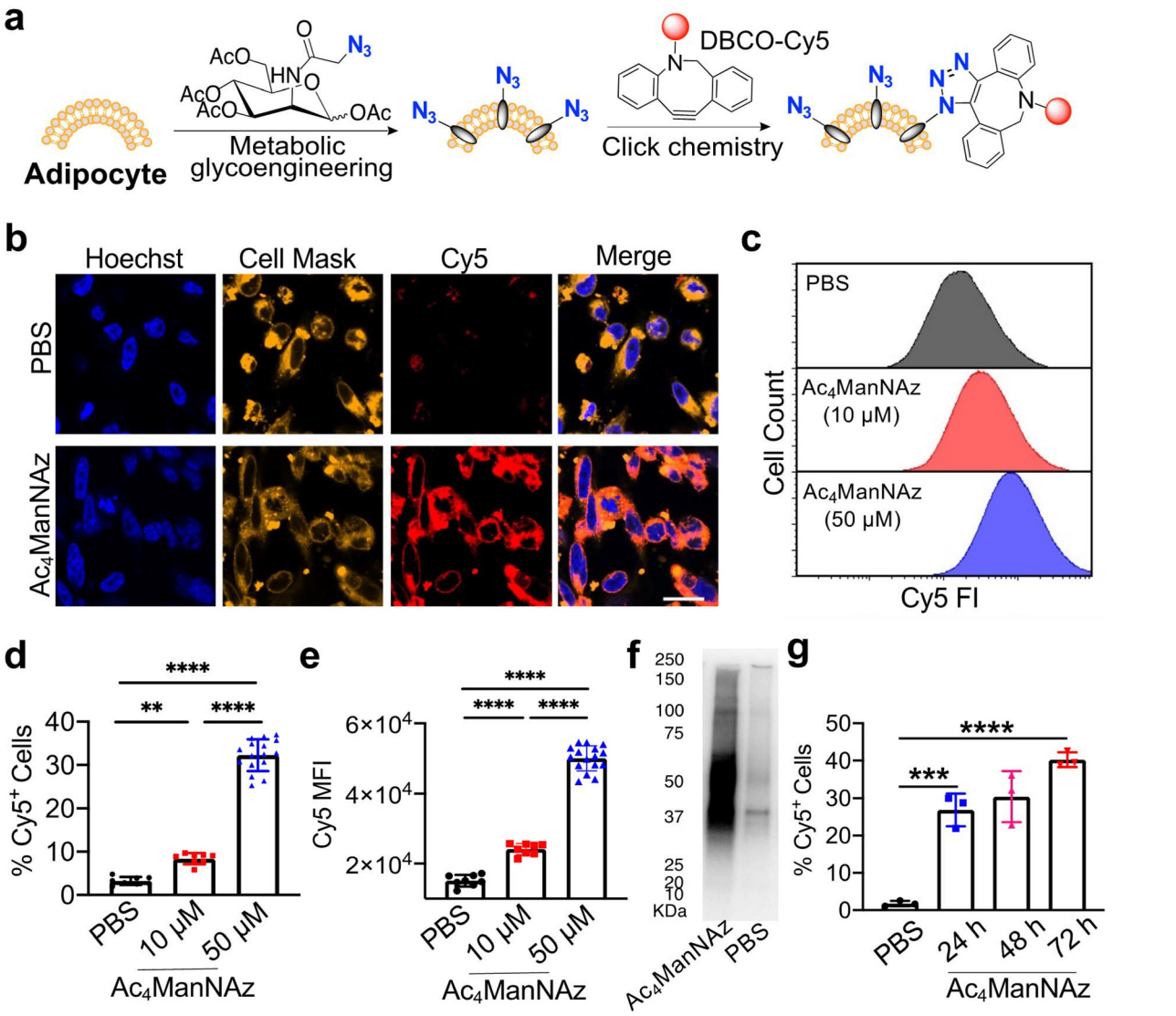

Fig. 1 *In vitro* metabolic glycan labeling of adipocytes. (a) Schematic illustration of metabolic labeling of adipocytes and subsequent detection of expressed azido groups *via* click chemistry. (b) CLSM images of adipocytes treated with $Ac_4ManNAz$ or PBS for three days and then incubated with DBCO-Cy5 for 30 min. The cell membrane and nucleus were stained with Cell Mask Orange (orange) and Hoechst 33342 (blue), respectively. Scale bar, 20 μm. (c) Representative flow cytometry histograms of adipocytes. (d) Percentage of azide$^+$ adipocytes after 3-day incubation with $Ac_4ManNAz$ ($N > 8$). (e) Mean Cy5 fluorescence intensity of adipocytes in (d) ($N > 8$). (f) Western blot analysis of adipocytes pretreated with $Ac_4ManNAz$ or PBS for three days. Azido-tagged proteins were biotinylated and then detected by using a streptavidin–horseradish peroxidase conjugate. (g) Percentage of Cy5$^+$ adipocytes after treatment with 50 μM $Ac_4ManNAz$ for 24, 48, and 72 h, respectively, and incubation with DBCO-Cy5 for 30 min ($N = 3$). All the numerical data are presented as mean ± SD ($0.01 < {}^*P \leq 0.05$; $0.001 < {}^{**}P \leq 0.01$; $0.0001 < {}^{***}P \leq 0.001$, $^{****}P \leq 0.0001$).

during macrophage–adipocyte interactions.[40–45] However, facile strategies to manipulate macrophage-mediated phagocytosis of adipocytes are still lacking.[46] We envision that the metabolic labeling and targeting technology will enable the conjugation of signaling molecules onto the surface of adipocytes for the orchestration of adipocyte–macrophage interactions. We demonstrate that through conjugating signaling molecules, including adiponectin (ACRP), calreticulin (CRT), mannose-binding lectin 2 (MBL-2) and milk fat globule-EGF factor 8 protein (MFG-E8), onto the surfaces of adipocytes, the phagocytosis of adipocytes by macrophages can be tuned.

Results and discussion

In vitro metabolic glycan labeling of adipocytes

We first studied whether tetraacetyl-*N*-azidoacetylmannosamine (Ac_4ManNAz), a commonly used labeling agent, can metabolically label adipocytes *in vitro*. Adipocytes were differentiated from 3T3-L1 fibroblasts and exhibited their expected morphology and lipid droplet structures (Fig. S1†). Fluorescence imaging of Nile red-stained 3T3-L1 differentiated adipocytes also confirmed the lipid droplet structures (Fig. S2†). Adipocytes were then incubated with a maintenance medium supplemented with or without Ac_4ManNAz for three days, followed by the detection of cell-surface azido groups *via* DBCO-Cy5 (Fig. 1a). Compared to the control adipocytes, adipocytes treated with Ac_4ManNAz showed a significantly enhanced Cy5 fluorescence signal on the cell membrane (Fig. 1b), indicating the successful metabolic labeling of cells with azido groups. Flow cytometry analysis confirmed the much higher Cy5 fluorescence intensity of Ac_4ManNAz-treated adipocytes than the control adipocytes (Fig. 1c–e). In addition, the labeling efficiency increased with the concentration of Ac_4ManNAz (Fig. 1d and e). It is noteworthy that 3-day incubation with 50 μM Ac_4ManNAz did not induce any noticeable cytotoxicity towards 3T3-L1-differentiated adipocytes (Fig. S3†).

To further confirm the metabolic tagging of cell-surface glycoproteins, we performed western blot analysis of adipocytes pretreated with or without Ac_4ManNAz for three days. Azido-labeled proteins in cell lysates were biotinylated by reacting with biotin-PEG_4-phosphine and then detected by the streptavidin–horseradish peroxidase (HRP) conjugate. As a result, adipocytes treated with Ac_4ManNAz showed significantly higher protein signals than cells without Ac_4ManNAz treatment (Fig. 1f), demonstrating the successful azido tagging of proteins. To better understand the metabolic labeling kinetics, we incubated 3T3-L1-differentiated adipocytes with Ac_4ManNAz for 24, 48, and 72 h, respectively, and detected the cell-surface azido groups using DBCO-Cy5 at each time point. A noticeable number of azido groups were already expressed by adipocytes within 24 h, with a negligible difference between 24 h and 48 h. At 72 h, a slightly increased expression of azido groups by adipocytes was detected (Fig. 1g). These experiments demonstrated that Ac_4ManNAz can metabolically label adipocytes with azido groups in a concentration-dependent manner, and a noticeable number of azido groups can be expressed within 24 h.

Stability of cell-surface azido tags

We next studied the stability of expressed azido groups. After incubating adipocytes with Ac_4ManNAz for three days, cells were transferred to fresh media without Ac_4ManNAz and cultured for 24, 48, and 96 h, respectively, followed by the detection of surface azido groups *via* DBCO-Cy5. The density of cell-surface azido groups showed a significant reduction at 24 h, but was well maintained from 24 h to 96 h (Fig. 2a–c). At 96 h,

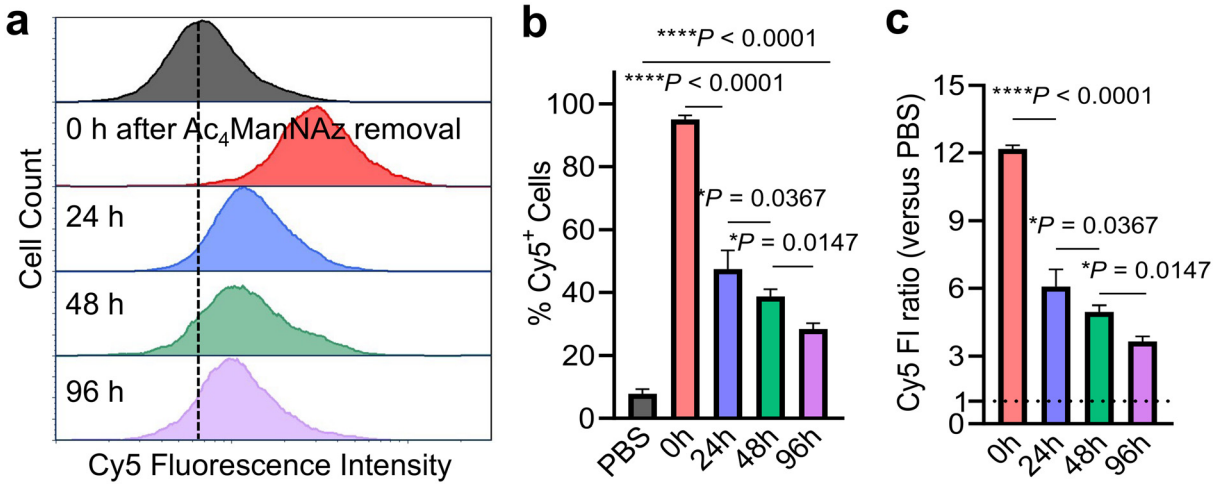

Fig. 2 Azido groups expressed on adipocytes were maintained for over 96 h. (a–c) Adipocytes were pretreated with Ac_4ManNAz for 3 days and then transferred to fresh blank media. At 0, 24, 48, or 96 h post-Ac_4ManNAz removal, cell-surface azido groups were detected by using DBCO-Cy5. Adipocytes pretreated with PBS and incubated with DBCO-Cy5 were used as negative controls. (a) Representative Cy5 histograms of adipocytes at 0, 24, 48, and 96 h, respectively. (b) Percentage of $Cy5^+$ adipocytes at different times ($N = 4$). (c) Cy5 fluorescence intensity ratios (*versus* PBS group) at different times ($N = 4$) ($0.01 < {}^*P \leq 0.05$; $0.001 < {}^{**}P \leq 0.01$; $0.0001 < {}^{***}P \leq 0.001$, $^{****}P \leq 0.0001$).

an ~3.6-fold Cy5 signal was still observed in Ac_4ManNAz-treated adipocytes, in comparison with the control adipocytes (Fig. 2c). This aligns with the proliferation rate of 3T3-L1-differentiated adipocytes and supports our hypothesis that lowly proliferative adipocytes can maintain the level of expressed azido groups over an extended time compared to highly proliferative cancer cells and immune cells.

Conjugation and membrane retention of DBCO-cargo

Azido-labeled adipocytes enable conjugation of DBCO-molecules *via* click chemistry, but the membrane retention and cell uptake rate of conjugated molecules remain elusive. Using DBCO-Cy5 as a model compound, we monitored the cellular internalization of DBCO-Cy5 by azido-labeled adipocytes *via* live-cell fluorescence imaging (Fig. 3a). Adipocytes were pre-treated with Ac_4ManNAz for three days, conjugated with DBCO-Cy5, and transferred to fresh media for live-cell imaging. A clear and uniform Cy5 signal was observed on the cell membrane at 0 h (Fig. 3a). Over time, cell-surface Cy5 gradually entered cells (Fig. 3a). To better compare the cellular micro-distribution of Cy5 at different times, we averaged and plotted the fluorescence pixels from the surface to the center of at least 50 adipocytes per time point, which indicates

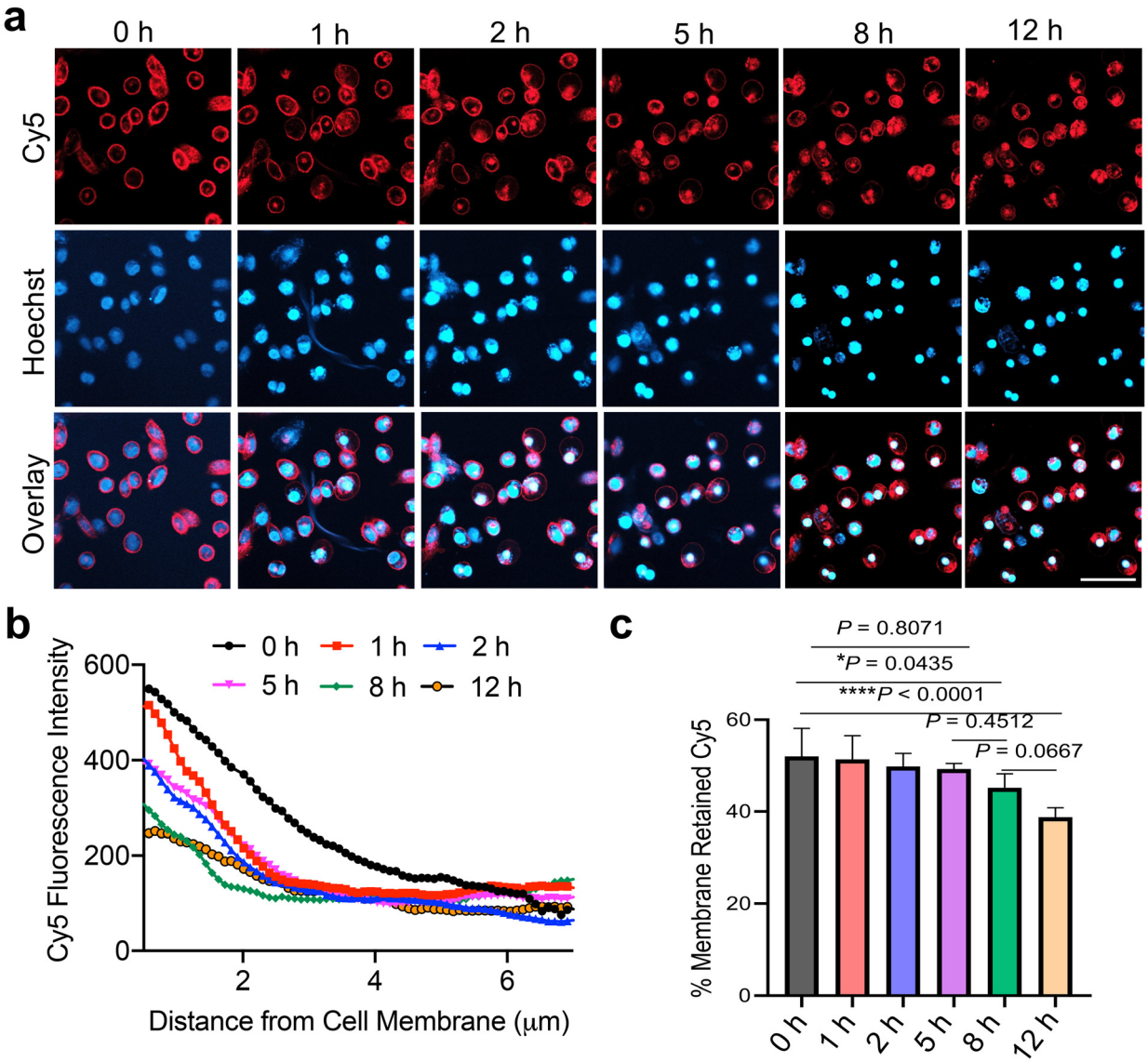

Fig. 3 Conjugated cargo is retained well on the adipocyte membrane. (a–c) Adipocytes were pretreated with Ac_4ManNAz for 3 days and then incubated with DBCO-Cy5 for 30 min. After removing DBCO-Cy5, the cells were monitored by fluorescence imaging. (a) Representative CLSM images of adipocytes at different times post the removal of DBCO-Cy5. Cell nuclei were stained with Hoechst 33342 (cyan). Scale bar: 50 μm. (b) Averaged Cy5 fluorescence intensity distribution over the longitudinal axis of cells from (a). (c) Percentage of membrane-bound Cy5 at different times post the removal of DBCO-Cy5, which is calculated by dividing the Cy5 fluorescence counts of 0–2 μm by the total fluorescence counts (0–7 μm) (N = 4). All the numerical data are presented as mean ± SD ($0.01 < {}^{*}P \leq 0.05$; $0.001 < {}^{**}P \leq 0.01$; $0.0001 < {}^{***}P \leq 0.001$, ${}^{****}P \leq 0.0001$).

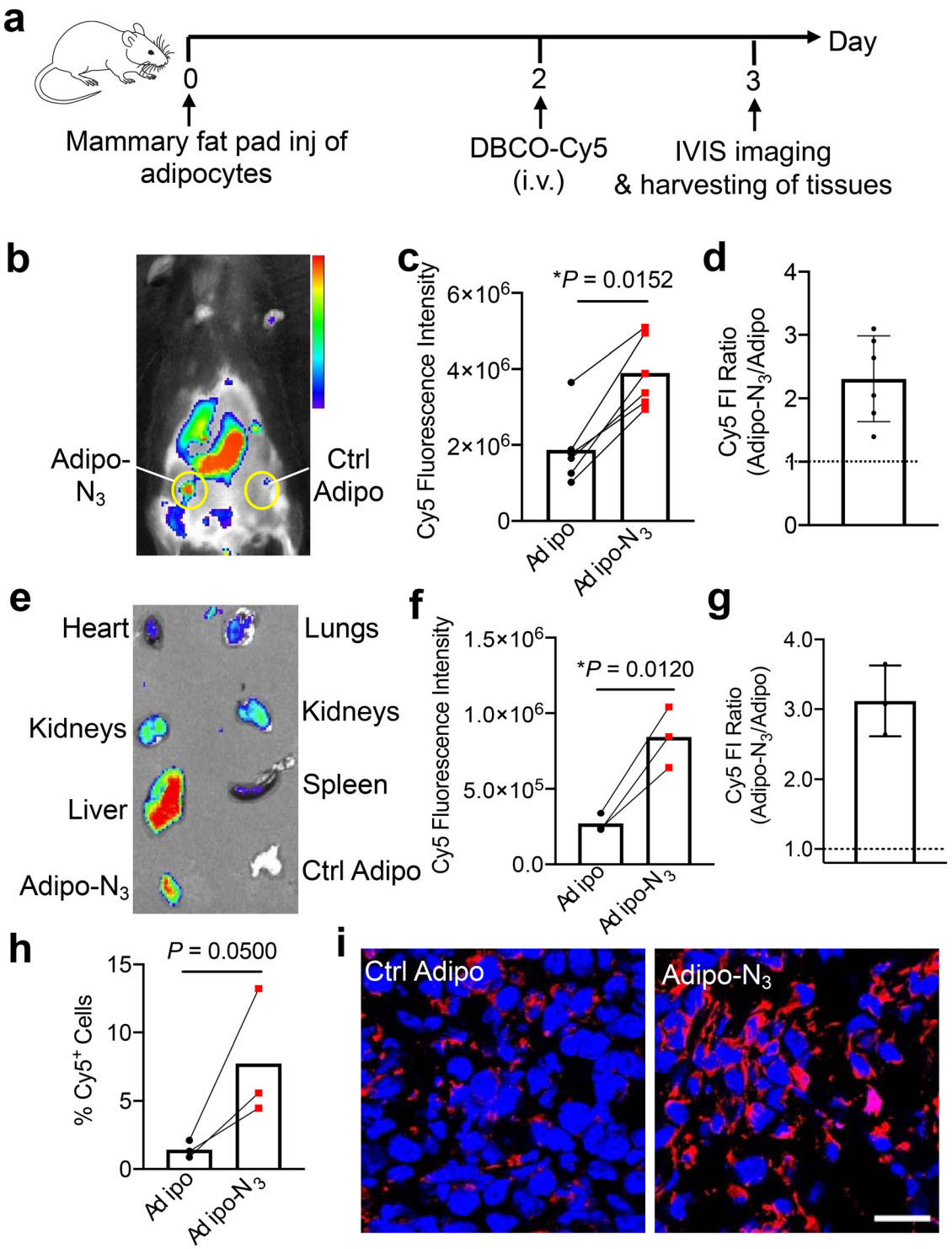

Fig. 4 Azido-labeled adipocytes can mediate targeted conjugation of DBCO-cargo *in vivo*. (a) Timeframe of the *in vivo* adipocyte targeting study. 3T3-L1-differentiated adipocytes were pretreated with $Ac_4ManNAz$ for three days and injected into the left mammary fat pad of mice, while the control adipocytes without azido labeling were injected into the right mammary fat pad. After 48 h, DBCO-Cy5 was intravenously injected. (b) Representative *in vivo* fluorescence imaging of mice at 24 h post-injection of DBCO-Cy5. (c) Cy5 fluorescence intensity of azido-labeled adipocytes or the control adipocytes extracted from the *in vivo* whole-body imaging (N = 5). (d) Ratio of Cy5 fluorescence intensity from (c) (N = 5). (e) Representative *ex vivo* fluorescence imaging of the harvested tissues. (f) Cy5 fluorescence intensity of the harvested fat tissues containing azido-labeled adipocytes or the control adipocytes (N = 3). (g) Ratio of Cy5 fluorescence intensity from (f) (N = 3). (h) Percentage of $Cy5^+$ cells isolated from fat tissues containing azido-labeled adipocytes or the control adipocytes, as determined by flow cytometry (N = 3). (i) CLSM image of the harvested fat tissues containing azido-labeled adipocytes. Cell nuclei were stained with Hoechst 33342 (blue). Scale bar: 20 μm. All the numerical data are presented as mean ± SD ($0.01 < *P \leq 0.05$; $0.001 < **P \leq 0.01$; $0.0001 < ***P \leq 0.001$, $****P \leq 0.0001$).

that the Cy5 signal was mainly located on the cell membrane at 0 h and gradually shifted to the cell center over time (Fig. 3b). Further quantification of membrane-bound Cy5 (0–2 μm) and internalized Cy5 (2–7 μm) indicates that the conjugated Cy5 stayed close to the membrane for at least 5 h (Fig. 3c). At 12 h, the percentage of surface Cy5 (~40%) only showed a slight decrease from that observed at the initial time point (~50% at 0 h) (Fig. 3c), demonstrating the long membrane retention of the conjugated Cy5. This could be attributed to the low endocytic and metabolic activities of mature adipocytes.

In vivo targeting of azido-labeled adipocytes

We next studied whether azido-labeled adipocytes can mediate targeted conjugation of DBCO-cargo *via* click chemistry *in vivo*. Azido-labeled adipocytes, as obtained *via in vitro* incubation of 3T3-L1 differentiated adipocytes with Ac_4ManNAz, were inoculated into the left mammary fat pad of mice. Control adipocytes without Ac_4ManNAz treatment were inoculated into the right mammary fat pad. After 48 h, DBCO-Cy5 was intravenously injected (Fig. 4a). *In vivo* imaging of the live mice at 24 h post-injection of DBCO-Cy5 showed a significantly higher

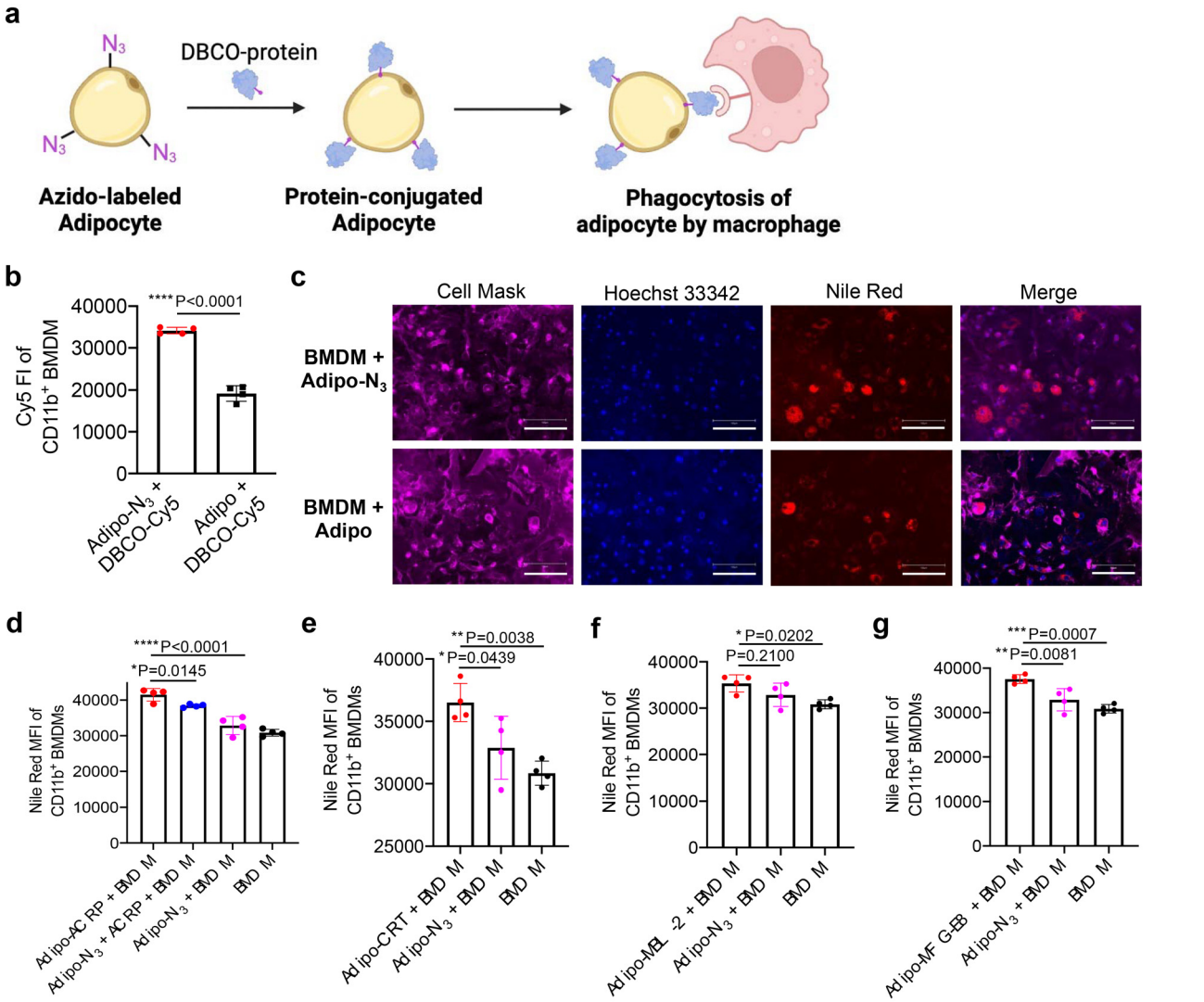

Fig. 5 Modulation of macrophage-mediated phagocytosis of adipocytes. (a) Schematic illustration of adipocytes conjugated with DBCO-proteins (signaling molecules) being phagocytosed by macrophages. (b) Cy5 MFI of macrophages after being cocultured with adipocytes that were treated with Ac_4ManNAz or PBS and incubated with DBCO-Cy5. (c) Fluorescence images of macrophages cocultured with adipo-N_3 or adipo. Cells were stained with CellMask (cell membrane) and Hoechst 33342 (nucleus). Adipocytes were pre-stained with Nile red. Scale bar: 150 μm. (d) Nile red MFI staining of macrophages after being cocultured with ACRP-conjugated adipocytes, the mixture of adipo-N_3 and ACRP, adipo-N_3, or PBS (N = 4). Adipocytes were pre-stained with Nile red. (e) Nile red MFI staining of macrophages after being cocultured with calreticulin-conjugated adipocytes, adipo-N_3, or PBS (N = 4). Adipocytes were pre-stained with Nile red. (f) Nile red MFI staining of macrophages after being cocultured with MBL-2-conjugated adipocytes, adipo-N_3, or PBS. Adipocytes were pre-stained with Nile red (N = 4). (g) Nile red MFI staining of macrophages after being cocultured with MFG-E8-conjugated adipocytes, adipo-N_3, or PBS (N = 4). Adipocytes were pre-stained with Nile red. All the numerical data are presented as mean ± SD ($0.01 < {}^{*}P \leq 0.05$; $0.001 < {}^{**}P \leq 0.01$; $0.0001 < {}^{***}P \leq 0.001$, $^{****}P \leq 0.0001$).

Cy5 accumulation in Ac_4ManNAz-pretreated adipocytes than in control adipocytes (Fig. 4b–d). Subsequent *ex vivo* imaging also showed a much higher Cy5 signal in Ac_4ManNAz-pretreated adipocytes than control adipocytes, with ~3-fold difference in Cy5 fluorescence intensity (Fig. 4e–g). Flow cytometry analysis of retrieved adipocytes showed a significantly higher fraction of $Cy5^+$ population in Ac_4ManNAz-pretreated adipocytes than in control adipocytes (Fig. 4h). Confocal imaging of isolated adipocytes also showed an enhanced Cy5 signal in Ac_4ManNAz-pretreated adipocytes than the control adipocytes (Fig. 4i). These experiments demonstrated that azido-labeled adipocytes enable *in vivo* targeted conjugation of DBCO-cargos *via* efficient click chemistry.

Modulation of adipocyte–macrophage interactions

We next explored whether signaling molecules including ACRP, CRT, MBL-2, and MFG-E8 can be covalently conjugated onto azido-labeled adipocytes to manipulate adipocyte–macrophage interactions (Fig. 5a). Prior to that, we first confirmed the ability of bone marrow-derived macrophages (BMDMs), which were differentiated from murine bone marrow cells for 6 days (Fig. S4†) to phagocytose adipocytes *via* two methods. In one method, adipocytes were pretreated with or without Ac_4ManNAz, incubated with DBCO-Cy5, and then co-incubated with BMDMs for 16 h. Compared to the control adipocytes, Ac_4ManNAz-pretreated adipocytes resulted in a higher Cy5 fluorescence intensity of BMDMs (Fig. 5b), demonstrating the successful azido labeling of adipocytes, conjugation of DBCO-Cy5, and phagocytosis of Cy5-conjugated adipocytes by BMDMs. In the other method, adipocytes were pre-stained with Nile red and then incubated with BMDMs. Both Ac_4ManNAz-pretreated adipocytes (*i.e.*, azido-labeled adipocytes) and unlabeled adipocytes managed to be internalized by BMDMs (Fig. 5c).

We next synthesized DBCO-functionalized ACRP, CRT, MBL-2, and MFG-E8 *via* amine-carboxyl chemistry. Matrix-assisted laser desorption/ionization (MALDI) spectrometry confirmed the successful synthesis of DBCO-ACRP (Fig. S5†), DBCO-CRT (Fig. S6†), DBCO-MBL-2 (Fig. S7†), and DBCO-MFG-E8 (Fig. S8†). To study whether the conjugation of these signaling molecules can tune the phagocytosis of adipocytes by macrophages, 3T3-L1-differentiated adipocytes were treated with Ac_4ManNAz or PBS, conjugated with DBCO-ACRP, DBCO-CRT, DBCO-MBL-2, and DBCO-MFG-E8, respectively, stained with Nile red, and co-incubated with BMDMs. Compared to BMDMs treated with PBS or adipocytes alone, BMDMs treated with ACRP-conjugated adipocytes showed enhanced Nile red fluorescence intensity, indicating an enhanced phagocytosis process (Fig. 5d). Compared to the mixture of adipocytes and ACRP, ACRP-conjugated adipocytes also induced an enhanced phagocytosis process by BMDMs (Fig. 5d). Compared to adipocytes alone, CRT-conjugated adipocytes also resulted in an improved phagocytosis process by BMDMs (Fig. 5e). The surface conjugation of MBL-2, though, did not enhance the phagocytosis process of adipocytes by macrophages (Fig. 5f). The surface conjugation of MFG-E8 to adipocytes managed to improve the phagocytosis of adipocytes by BMDMs (Fig. 5g). These experiments demonstrated the promise of conjugating signaling molecules to adipocytes, *via* the metabolic labeling and targeting approach, for the orchestration of adipocyte–macrophage interactions. It is noteworthy that different signaling molecules may exhibit varied effects on the modulation of macrophage phagocytotic activities. For example, adiponectin has been reported to modulate the phagocytotic activity of macrophages differently. While it was shown that adiponectin promotes the phagocytosis of early apoptotic bodies by macrophages,[47] other findings suggest that adiponectin reduces the phagocytotic activity of mature macrophages, possibly playing a role in its protective effect against inflammation.[48,49] Nevertheless, our metabolic labeling and conjugation method provides a unique approach for displaying phagocytotic modulators on the surface of target cells and probing the interaction between macrophages and the target cells.

Conclusion

To summarize, we have reported the successful metabolic glycan labeling of adipocytes, elucidated the metabolic labeling kinetics of adipocytes, understood the membrane retention time of DBCO molecules covalently conjugated to azido-labeled adipocytes, demonstrated the *in vivo* targeting of adipocytes *via* click chemistry, and validated the feasibility to orchestrate adipocyte–macrophage interactions *via* the surface conjugation of signaling molecules onto adipocytes. This adipocyte tagging and targeting technology will not only greatly facilitate the development of adipocyte-based cell therapies, but also enable the probing of the interactions between adipocytes and other cells in the context of cancer, diabetes, and many other diseases.

Methods

Materials and instrumentation

D-Mannosamine hydrochloride, DBCO-Cy5, sodium azide, chloroacetic anhydride, acetic anhydride, cisplatin, DBCO-sulfo-amine, L-luciferin potassium, octyl isocyanate, MTT, CCK-8 kit, and other chemical reagents were purchased from Sigma-Aldrich (St Louis, MO, USA) unless otherwise noted. High-performance liquid chromatography (HPLC) analysis was performed on a Shimadzu CBM-20A system (Shimadzu, Kyoto, Japan) equipped with an SPD-20A PDA detector (190–800 nm), an RF-20A fluorescence detector, and an analytical C18 column (Shimadzu, 3 μm, 50 × 4.6 mm, Kyoto, Japan). Preparative HPLC was performed on a CombiFlash® Rf system (Teledyne ISCO, Lincoln, NE, USA) equipped with a RediSep® Rf HP C18 column (Teledyne ISCO, 30 g, Lincoln, NE, USA). Lyophilization was conducted in a Labconco FreeZone lyophilizer (Kansas City, MO, USA). Nuclear magnetic resonance (NMR) spectra were recorded using a Varian U500 (500 MHz) or VXR500 (500 MHz), or a Bruker Carver B500 (500 MHz) spectrometer. Electrospray ionization (ESI) mass spectra were

recorded using a Waters ZMD Quadrupole instrument (Waters, Milford, MA, USA). Confocal laser scanning microscopy (CLSM) images were taken by using a Zeiss LSM 700 or LSM 880 confocal microscope (Carl Zeiss, Thornwood, NY, USA). Western blotting of protein bands were imaged using an ImageQuant LAS 4000 gel imaging system (GE, Pittsburgh, PA, USA). *In vivo* and *ex vivo* images of animals and tissues were taken using a Bruker *in vivo* imaging system (Bruker, Billerica, MA, USA). Frozen tumor tissues were embedded with an optimum cutting temperature (OCT) compound (Sakura Finetek USA, Torrance, CA, USA), sectioned by using a Leica CM3050S cryostat, and mounted onto glass slides. Nile Red (Invitrogen™ N1142) and 3T3 differentiation kit (Abcam ab287843) were purchased from Fisher Scientific. Recombinant Mouse Adiponectin was purchased from R&D Systems Inc, Calreticulin/CALR Protein and MFG-E8 Protein were from Medchemexpress LLC, Mouse MBL-2 was from Fisher Scientific Company LLC. Flow cytometry analysis was conducted by using an Attune NxT flow cytometer and analyzed using FlowJo V10.8.1 software. Matrix-assisted laser desorption ionization (MALDI) was determined by using a Bruker Daltonics UltrafleXtreme MALDI TOFTOF.

Cell line and animals

The 3T3-L1 cell line was purchased from the American Type Culture Collection (Manassas, VA, USA). 3T3-L1 cells were cultured in DMEM/F12 media containing 10% bovine calf serum (Gibco), 100 units per mL penicillin G and 100 μg mL^{-1} streptomycin (Invitrogen, Carlsbad, CA, USA) at 37 °C in a 5% CO_2 humidified incubator. Female C57BL/6 mice and BALB/c mice were purchased from the Jackson Laboratory (Bar Harbor, ME, USA). Feed and water were made available *ad libitum*. Artificial light was provided under a 12 h/12 h cycle. All procedures involving animals were conducted in compliance with the National Institutes of Health and Institutional guidelines with approval from the Institutional Animal Care and Use Committee at the University of Illinois at Urbana-Champaign.

Synthesis of Ac_4ManNAz

To a solution of D-mannosamine hydrochloride (1.00 g, 4.64 mmol) in methanol (10 mL) was dropwise added 0.5 N sodium methoxide in methanol (9.3 mL, 4.64 mmol) at 0 °C. The mixture was stirred at room temperature for 30 min. Triethylamine (0.47 g, 4.64 mmol) and chloroacetic anhydride (0.95 g, 5.57 mmol, 95%) were then added. The reaction mixture was stirred overnight, followed by the addition of H_2O (3 mL) and sodium azide (1.21 g, 18.56 mmol). After being stirred overnight at 65 °C, the precipitate was filtered out and the filtrate was concentrated. The residue was suspended in pyridine (15 mL), followed by the addition of 4-dimethylaminopyridine (56.8 mg, 0.47 mmol) and acetic anhydride (3.79 g, 37.12 mmol). The mixture was stirred overnight at room temperature, and then quenched with methanol. After the removal of solvents, the residue was dissolved in ethyl acetate and washed successively with HCl (1 M), brine, and saturated $NaHCO_3$ (aq). The organic layer was dried over Na_2SO_4 and filtered. The filtrate was concentrated, and the crude product was purified by silica gel column chromatography to yield a white foam (1.40 g, 70% yield). LRMS (ESI) *m*/*z*: calculated for $C_{16}H_{22}N_4O_{10}Na$ $[M + Na]^+$ 453.1, found 453.1. ^1H NMR ($CDCl_3$, 500 MHz): δ (ppm) 6.66 & 6.60 (d, J = 9.0 Hz, 1H, C(O)N*H*CH), 6.04 & 6.04 (d, 1H, J = 1.9 Hz, NHCHC*H*O), 5.32–5.35 & 5.04–5.07 (dd, J = 10.2, 4.2 Hz, 1H, $CH_2CHCHCH$), 5.22 & 5.16 (t, J = 9.9 Hz, 1H, $CH_2CHCHCH$), 4.60–4.63 & 4.71–4.74 (m, 1H, NHC*H*CHO), 4.10–4.27 (m, 2H, $CH_2CHCHCH$), 4.07 (m, 2H, $C(O)CH_2N_3$), 3.80–4.04 (m, 1H, $CH_2CHCHCH$), 2.00–2.18 (s, 12H, $CH_3C(O)$). ^{13}C NMR ($CDCl_3$, 500 MHz): δ (ppm) 170.7, 170.4, 170.3, 169.8, 168.6, 168.3, 167.5, 166.9, 91.5, 90.5, 73.6, 71.7, 70.5, 69.1, 65.3, 65.1, 62.0, 61.9, 52.8, 52.6, 49.9, 49.5, 21.1, 21.0, 21.0, 20.9, 20.9, 20.9, 20.8.

Differentiation and characterization of 3T3-L1 cells

3T3-L1 cells were cultured and differentiated following the 3T3-L1 differentiation kit protocol (ab287843). Briefly, cells were cultured to 70% confluency in a full DMEM/F12 medium in a 12 well plate. The medium was replaced and the cells were cultured for another 48 hours. Then, the medium was changed to a differentiation medium (full DMEM/F12 with a differentiation cocktail). Cells were incubated for 72 h. After removing the differentiation medium, a maintenance medium (10 μg mL^{-1} insulin in full DMEM/F12) was added. Cells were incubated for another 4–7 days. The medium was changed every 48 h. Lipid droplet structures were visualized under light microscopy, confirming the maturation of adipocytes. In addition, Nile red staining of the lipid content was performed. Briefly, Nile red stock solution (1 mg mL^{-1} in DMSO) was diluted with the culture medium to an optimal working concentration of 10 μg mL^{-1} before the experiment. Adipocytes were incubated with 10 μg mL^{-1} Nile red for 15 min at 37 °C and then washed twice with PBS. Fluorescence images of Nile red-stained adipocytes were then taken under a fluorescence microscope with the RFP channel.

Flow cytometry analysis of adipocytes

3T3-L1-differentiated adipocytes were incubated with Ac_4ManNAz (50 μM) at 37 °C for 24, 48, or 72 h. After washing with PBS three times, cells were incubated with DBCO-Cy5 (20 μM) for 30 min. Cells were then lifted with trypsin, resuspended in FACS buffer, and analyzed by using a flow cytometer.

Viability test of adipocytes

3T3-L1-differentiated adipocytes were incubated with Ac_4ManNAz of different concentrations (0, 20, 50, 100 and 200 μM) at 37 °C for 72 h. After washing with PBS three times, cells were lifted, stained with a fixable viability dye according to the manufacturer's suggestions, and analyzed by using a flow cytometer.

Stability of cell-surface azido groups

3T3-L1-differentiated adipocytes were incubated with Ac_4ManNAz (50 μM) at 37 °C for 72 h. After washing with PBS

three times, cells were cultured in fresh blank media for 24 h, 48 h, and 96 h, respectively, and then incubated with DBCO-Cy5 (20 μM) for 30 min. Cells were then lifted with trypsin, suspended in FACS buffer, and analyzed by using a flow cytometer.

Cell uptake of conjugated DBCO-Cy5

3T3-L1-differentiated adipocytes were incubated with Ac_4ManNAz (50 μM) at 37 °C for 72 h. After washing with PBS three times, cells were incubated with DBCO-Cy5 (20 μM) for 30 min, and cell nuclei were stained with Hoechst 33342. After washing, cells were imaged under a fluorescence microscope to monitor the cellular internalization of conjugated DBCO-Cy5.

Western blot analysis of azido-labeled adipocytes

The metabolic glycan labeling procedure is described above. After washing with PBS, cells were lysed with lysis buffer (50 mM Tris-HCl, 1% SDS, pH 7.4), and the lysate was incubated at 4 °C for 30 min. Following debris removal by centrifugation at 10 000 rpm, the protein concentration of cell lysates was quantified using a standard BCA assay. After adjusting the amount of proteins, iodoacetamide was added to the lysates and incubated at 37 °C for 1 h to block the free thiol groups. DBCO-PEG_4-biotin was then added to the mixture and incubated overnight at 37 °C. The protein mixture was mixed with a sample buffer, heated at 95 °C for 10 min, subjected to electrophoresis on a 4–20% gel (MiniPROTEAN TGX precast gel, Bio-Rad), and then transferred to the PVDF membrane using a trans-Blot Turbo™ Transfer System (Bio-Rad). The protein concentration was confirmed by reversible Ponceau S staining (Sigma-Aldrich, P7170). The membrane was incubated with streptavidin–HRP (Invitrogen) at room temperature for 1 h and washed with TBST buffer. The blots were developed with an ECL western blotting substrate and imaged with an LAS 4010 luminescence image analyzer.

In vivo targeting of 3T3-L1-differentiated adipocytes

3T3-L1-differentiated adipocytes were incubated with Ac_4ManNAz (50 μM) or PBS for 3 days. Cells were rinsed with PBS three times and then lifted with trypsin. 10^7 azido-labeled adipocytes were inoculated into the fat pad under the mammary gland at the left flank of female C57BL/6 mice. Unlabeled adipocytes were inoculated into the right flank as the control. After 48 h, DBCO-Cy5 (5 mg kg^{-1}) was intravenously administered. Mice were imaged by using the IVIS imaging system with an excitation/emission filter of 640/700 nm. After euthanizing the mice, major organs including the fat tissue with grafted adipocytes were harvested and imaged *ex vivo*. The fluorescence intensity at the selected ROIs was quantified using IVIS imaging software.

Synthesis of DBCO-proteins

ACRP, CRT, MBL-2, or MFG-E8 was mixed with DBCO-sulfo-NHS in an Eppendorf tube and shaken at 4 °C overnight. The mixture was then ultracentrifuged by using an Amicon filter (3.5 kDa MWCO) and washed with deionized water at least three times. Aliquots of the purified proteins were analyzed *via* matrix-assisted laser desorption/ionization (MALDI) spectrometry.

Conjugation of signaling molecules onto adipocytes

3T3-L1-differentiated adipocytes were treated with Ac_4ManNAz (50 μM) for 72 h during the last three days of the culture period. Cells were then washed three times with PBS. A maintenance medium containing 10 μg ml^{-1} DBCO-proteins (signaling molecules) was added and cells were incubated for 2 h. Nile red was added into the medium 30 min before the end of conjugation to label the lipid (final concentration: 2 μM). Adipocytes were then washed two times with PBS before being used.

Differentiation of bone marrow-derived macrophages (BMDMs)

Bone marrow was isolated from the tibia and femur of C57BL/6 mice (6–8 weeks old). Bone marrow cells were counted after red blood cell lysis and seeded with 1×10^6 cells per mL in BMDM media (DMEM/F12 supplemented with 10% FBS, 100 U ml^{-1} penicillin, 100 μg ml^{-1} streptomycin, 20 ng ml^{-1} M-CSF). On day 3, an additional BMDM medium (half of the original volume) was added to the plate. On day 6, BMDMs were collected for use.

Coculture of adipocytes and BMDMs

After conjugation of a signaling molecule, adipocytes were lifted with trypsin and centrifuged, and then resuspended in maintenance medium. Adipocytes were then stained with Nile red and added on top of BMDMs at a ratio of 1 : 1. The cells were cocultured for 24 hours in the maintenance medium. At the end of coculture, cells were washed with PBS and excess adipocytes were removed by pipetting with PBS. The adherent macrophages were then lifted by gentle scraping. The macrophages were then washed and stained with antibodies for flow analysis.

Confocal imaging of adipocyte–macrophages

Macrophages were grown on coverslips pretreated with poly-D-lysine in 6-well plates. Adipocytes with or without metabolic labeling were stained with Nile red before being added into the macrophage culture dish. After 16 h of coculture, the unphagocytosed adipocytes were washed off by flushing with PBS at least three times; the remaining adherent macrophages were stained with Hoechst 33342 and CellMask far red plasma membrane stain according to the manufacturer's protocol. After washing with PBS 2–3 times, macrophages were transferred to 4% PFA solution and fixed for 15 min at room temperature. PFA was then removed, followed by a PBS wash. Then, coverslips with macrophages were mounted onto confocal slides using an antifade mounting medium.

Statistical analysis

Statistical analysis was performed using GraphPad Prism v6 and v8. Sample variance was tested using the *F* test. For

samples with equal variance, the significance between the groups was analyzed by a two-tailed Student's *t*-test. For samples with unequal variance, a two-tailed Welch's *t*-test was performed. For multiple comparisons, a one-way analysis of variance (ANOVA) with a *post hoc* Fisher's LSD test was used. The results were deemed significant at $0.01 < {}^{*}P \leq 0.05$ and $0.001 < {}^{**}P \leq 0.01$, highly significant at $^{***}0.01 < P \leq 0.001$, and extremely significant at $^{****}P < 0.0001$.

Data availability

Raw data can be accessed upon request and will be published at the Illinois Data Bank upon the acceptance of the manuscript.

Conflicts of interest

There are no conflicts to declare.

Acknowledgements

The authors would like to acknowledge the financial support from NSF DMR 2143673 CAR, NIH R01CA274738, NIH R21CA270872, and the start-up package from the Department of Materials Science and Engineering at the University of Illinois at Urbana-Champaign and the Cancer Center at Illinois. Research also was supported by the Cancer Scholars for Translational and Applied Research (C*STAR) Program sponsored by the Cancer Center at Illinois and the Carle Cancer Center under Award Number CST EP012023.

References

1 M. S. Desruisseaux, Nagajyothi, M. E. Trujillo, H. B. Tanowitz and P. E. Scherer, Adipocyte, adipose tissue, and infectious disease, *Infect. Immun.*, 2007, **75**(3), 1066–1078.
2 S. Laforest, J. Labrecque, A. Michaud, K. Cianflone and A. Tchernof, Adipocyte size as a determinant of metabolic disease and adipose tissue dysfunction, *Crit. Rev. Clin. Lab. Sci.*, 2015, **52**(6), 301–313.
3 S. Balaban, R. F. Shearer, L. S. Lee, M. van Geldermalsen, M. Schreuder, H. C. Shtein, R. Cairns, K. C. Thomas, D. J. Fazakerley and T. Grewal, Adipocyte lipolysis links obesity to breast cancer growth: adipocyte-derived fatty acids drive breast cancer cell proliferation and migration, *Cancer Metab.*, 2017, **5**(1), 1–14.
4 A. D. Attie and P. E. Scherer, Adipocyte metabolism and obesity, *J. Lipid Res.*, 2009, **50**, S395–S399.
5 F. Villarroya, R. Cereijo, J. Villarroya and M. Giralt, Brown adipose tissue as a secretory organ, *Nat. Rev. Endocrinol.*, 2017, **13**(1), 26–35.
6 D. F. Quail and A. J. Dannenberg, The obese adipose tissue microenvironment in cancer development and progression, *Nat. Rev. Endocrinol.*, 2019, **15**(3), 139–154.
7 J. O'Sullivan, J. Lysaght, C. L. Donohoe and J. V. Reynolds, Obesity and gastrointestinal cancer: the interrelationship of adipose and tumour microenvironments, *Nat. Rev. Gastroenterol. Hepatol.*, 2018, **15**(11), 699–714.
8 D. Hausman, M. DiGirolamo, T. Bartness, G. Hausman and R. Martin, The biology of white adipocyte proliferation, *Obes. Rev.*, 2001, **2**(4), 239–254.
9 H. Wang, L. Shen, X. Sun, F. Liu, W. Feng, C. Jiang, X. Chu, X. Ye, C. Jiang and Y. Wang, Adipose group 1 innate lymphoid cells promote adipose tissue fibrosis and diabetes in obesity, *Nat. Commun.*, 2019, **10**(1), 3254.
10 S. S. Sharath, J. Ramu, S. V. Nair, S. Iyer, U. Mony and J. Rangasamy, Human adipose tissue derivatives as a potent native biomaterial for tissue regenerative therapies, *Tissue Eng. Regener. Med.*, 2020, **17**(2), 123–140.
11 D. Wen, T. Liang, G. Chen, H. Li, Z. Wang, J. Wang, R. Fu, X. Han, T. Ci and Y. Zhang, Adipocytes Encapsulating Telratolimod Recruit and Polarize Tumor–Associated Macrophages for Cancer Immunotherapy, *Adv. Sci.*, 2023, **10**, 2206001.
12 D. Wen, J. Wang, G. Van Den Driessche, Q. Chen, Y. Zhang, G. Chen, H. Li, J. Soto, M. Liu and M. Ohashi, Adipocytes as anticancer drug delivery depot, *Matter*, 2019, **1**(5), 1203–1214.
13 R. Munteanu, A. Onaciu, C. Moldovan, A.-A. Zimta, D. Gulei, A. V. Paradiso, V. Lazar and I. Berindan-Neagoe, Adipocyte-based cell therapy in oncology: the role of cancer-associated adipocytes and their reinterpretation as delivery platforms, *Pharmaceutics*, 2020, **12**(5), 402.
14 E. Tsagkaraki, S. M. Nicoloro, T. DeSouza, J. Solivan-Rivera, A. Desai, L. M. Lifshitz, Y. Shen, M. Kelly, A. Guilherme and F. Henriques, CRISPR-enhanced human adipocyte browning as cell therapy for metabolic disease, *Nat. Commun.*, 2021, **12**(1), 1–17.
15 C.-H. Wang, M. Lundh, A. Fu, R. Kriszt, T. L. Huang, M. D. Lynes, L. O. Leiria, F. Shamsi, J. Darcy and B. P. Greenwood, CRISPR-engineered human brown-like adipocytes prevent diet-induced obesity and ameliorate metabolic syndrome in mice, *Sci. Transl. Med.*, 2020, **12**(558), eaaz8664.
16 C. R. Bertozzi and P. Wu, In vivo chemistry, *Curr. Opin. Chem. Biol.*, 2013, **17**(5), 717–718.
17 R. Xie, L. Dong, Y. Du, Y. Zhu, R. Hua, C. Zhang and X. Chen, In vivo metabolic labeling of sialoglycans in the mouse brain by using a liposome-assisted bioorthogonal reporter strategy, *Proc. Natl. Acad. Sci. U. S. A.*, 2016, **113**(19), 5173–5178.
18 R. Xie, L. Dong, R. Huang, S. Hong, R. Lei and X. Chen, Targeted imaging and proteomic analysis of tumor-associated glycans in living animals, *Angew. Chem., Int. Ed.*, 2014, **53**(51), 14082–14086.
19 E. S. C. R. Bertozzi, Cell Surface Engineering by a Modified Staudinger Reaction, *Science*, 2000, **287**(5460), 2007–2010.

20 C. Agatemor, M. J. Buettner, R. Ariss, K. Muthiah, C. T. Saeui and K. J. Yarema, Exploiting metabolic glycoengineering to advance healthcare, *Nat. Rev. Chem.*, 2019, **3**(10), 605–620.
21 J. Rong, J. Han, L. Dong, Y. Tan, H. Yang, L. Feng, Q. W. Wang, R. Meng, J. Zhao, S. Q. Wang and X. Chen, Glycan imaging in intact rat hearts and glycoproteomic analysis reveal the upregulation of sialylation during cardiac hypertrophy, *J. Am. Chem. Soc.*, 2014, **136**(50), 17468–17476.
22 P. V. Chang, J. A. Prescher, E. M. Sletten, J. M. Baskin, I. A. Miller, N. J. Agard, A. Lo and C. R. Bertozzi, Copper-free click chemistry in living animals, *Proc. Natl. Acad. Sci. U. S. A.*, 2010, **107**(5), 1821–1826.
23 J. A. Codelli, J. M. Baskin, N. J. Agard and C. R. Bertozzi, Second-Generation Difluorinated Cyclooctynes for Copper-Free Click Chemistry, *J. Am. Chem. Soc.*, 2008, **130**, 11486–11493.
24 A. K. Agrahari, P. Bose, M. K. Jaiswal, S. Rajkhowa, A. S. Singh, S. Hotha, N. Mishra and V. K. Tiwari, Introduction: Click Chemistry, *Chem. Rev.*, 2021, **121**(13), 7638–7956.
25 H. Wang, R. Wang, K. Cai, H. He, Y. Liu, J. Yen, Z. Wang, M. Xu, Y. Sun, X. Zhou, Q. Yin, L. Tang, I. T. Dobrucki, L. W. Dobrucki, E. J. Chaney, S. A. Boppart, T. M. Fan, S. Lezmi, X. Chen, L. Yin and J. Cheng, Selective in vivo metabolic cell-labeling-mediated cancer targeting, *Nat. Chem. Biol.*, 2017, **13**(4), 415–424.
26 H. Wang, M. C. Sobral, D. K. Y. Zhang, A. N. Cartwright, A. W. Li, M. O. Dellacherie, C. M. Tringides, S. T. Koshy, K. W. Wucherpfennig and D. J. Mooney, Metabolic labeling and targeted modulation of dendritic cells, *Nat. Mater.*, 2020, **19**(11), 1244–1252.
27 N. Geva-Zatorsky, D. Alvarez, J. E. Hudak, N. C. Reading, D. Erturk-Hasdemir, S. Dasgupta, U. H. von Andrian and D. L. Kasper, In vivo imaging and tracking of host-microbiota interactions via metabolic labeling of gut anaerobic bacteria, *Nat. Med.*, 2015, **21**(9), 1091–1100.
28 Y. Bo, Y. Jiang, K. Chen, K. Cai, W. Li, J. Roy, Y. Bao and J. Cheng, Targeting infected host cells in vivo via responsive azido-sugar mediated metabolic cell labeling followed by click reaction, *Biomaterials*, 2020, **238**, 119843.
29 M. K. Shim, H. Y. Yoon, J. H. Ryu, H. Koo, S. Lee, J. H. Park, J. H. Kim, S. Lee, M. G. Pomper, I. C. Kwon and K. Kim, Cathepsin B-Specific Metabolic Precursor for In Vivo Tumor-Specific Fluorescence Imaging, *Angew. Chem., Int. Ed.*, 2016, **55**(47), 14698–14703.
30 R. Wang, K. Cai, H. Wang, C. Yin and J. Cheng, A caged metabolic precursor for DT-diaphorase-responsive cell labeling, *Chem. Commun.*, 2018, **54**(38), 4878–4881.
31 H. Wang and D. J. Mooney, Metabolic glycan labelling for cancer-targeted therapy, *Nat. Chem.*, 2020, **12**(12), 1102–1114.
32 Y. Liu, K. Adu-Berchie, J. M. Brockman, M. Pezone, D. K. Y. Zhang, J. Zhou, J. W. Pyrdol, H. Wang, K. W. Wucherpfennig and D. J. Mooney, Cytokine conjugation to enhance T cell therapy, *Proc. Natl. Acad. Sci. U. S. A.*, 2023, **120**(1), e2213222120.
33 H. Kane and L. Lynch, Innate Immune Control of Adipose Tissue Homeostasis, *Trends Immunol.*, 2019, **40**(9), 857–872.
34 T. Chavakis, V. I. Alexaki and A. W. Ferrante Jr, Macrophage function in adipose tissue homeostasis and metabolic inflammation, *Nat. Immunol.*, 2023, **24**(5), 757–766.
35 V. J. Vieira-Potter, Inflammation and macrophage modulation in adipose tissues, *Cell. Microbiol.*, 2014, **16**(10), 1484–1492.
36 W. V. Trim and L. Lynch, Immune and non-immune functions of adipose tissue leukocytes, *Nat. Rev. Immunol.*, 2022, **22**(6), 371–386.
37 J. Y. Huh, Y. J. Park, M. Ham and J. B. Kim, Crosstalk between adipocytes and immune cells in adipose tissue inflammation and metabolic dysregulation in obesity, *Mol. Cells*, 2014, **37**(5), 365–371.
38 K. Lolmede, C. Duffaut, A. Zakaroff-Girard and A. Bouloumie, Immune cells in adipose tissue: key players in metabolic disorders, *Diabetes Metab.*, 2011, **37**(4), 283–290.
39 L. Boutens and R. Stienstra, Adipose tissue macrophages: going off track during obesity, *Diabetologia*, 2016, **59**(5), 879–894.
40 S. Y. Park and I. S. Kim, Engulfment signals and the phagocytic machinery for apoptotic cell clearance, *Exp. Mol. Med.*, 2017, **49**(5), e331.
41 P. Zelechowska, E. Kozlowska, J. Pastwinska, J. Agier and E. Brzezinska-Blaszczyk, Adipocytokine Involvement in Innate Immune Mechanisms, *J. Interferon Cytokine Res.*, 2018, **38**(12), 527–538.
42 A. Tajbakhsh, S. M. Gheibihayat, N. Karami, A. Savardashtaki, A. E. Butler, M. Rizzo and A. Sahebkar, The regulation of efferocytosis signaling pathways and adipose tissue homeostasis in physiological conditions and obesity: Current understanding and treatment options, *Obes. Rev.*, 2022, **23**(10), e13487.
43 A. Schcolnik-Cabrera, B. Oldak, M. Juarez, M. Cruz-Rivera, A. Flisser and F. Mendlovic, Calreticulin in phagocytosis and cancer: opposite roles in immune response outcomes, *Apoptosis*, 2019, **24**(3–4), 245–255.
44 L. Russo and C. N. Lumeng, Properties and functions of adipose tissue macrophages in obesity, *Immunology*, 2018, **155**(4), 407–417.
45 L. Fuentes, T. Roszer and M. Ricote, Inflammatory mediators and insulin resistance in obesity: role of nuclear receptor signaling in macrophages, *Mediators Inflammation*, 2010, **2010**, 219583.
46 A. B. Engin, Message Transmission Between Adipocyte and Macrophage in Obesity, in *Obesity and Lipotoxicity*, 2024, vol. 1460, pp. 273–295.
47 Y. Takemura, N. Ouchi, R. Shibata, T. Aprahamian, M. T. Kirber, R. S. Summer, S. Kihara and K. Walsh,

Adiponectin modulates inflammatory reactions via calreticulin receptor–dependent clearance of early apoptotic bodies, *J. Clin. Invest.*, 2007, **117**(2), 375–386.
48 R. Osman, P. Tacnet-Delorme, J.-P. Kleman, A. Millet and P. Frachet, Calreticulin Release at an Early Stage of Death Modulates the Clearance by Macrophages of Apoptotic Cells, *Front. Immunol.*, 2017, 8.
49 D. V. Krysko, K. S. Ravichandran and P. Vandenabeele, Macrophages regulate the clearance of living cells by calreticulin, *Nat. Commun.*, 2018, **9**(1), 4644.